



HARVARD MEDICAL SCHOOL



Children's Hospital Boston

# Accelerated Feature Based Registration for Electron Microscopy Images

A. Akselrod-Ballin, D. Bock,  
R. C. Reid, S. K. Warfield

# Outline

- **I Background**
  - Electron Microscopy
  - Related work
- **II Methods**
  - Dimensionality Reduction
  - Nearest Neighbor Search
  - Transformation Estimation (EM-ICP-NC)
- **III Experiments and Results**
- **V Summary**

# Outline

- **I Background**
  - **Electron Microscopy**
  - **Related work**
- **II Methods**
  - Dimensionality Reduction
  - Nearest Neighbor Search
  - Transformation Estimation (EM-ICP-NC)
- **III Experiments and Results**
- **IV Summary**

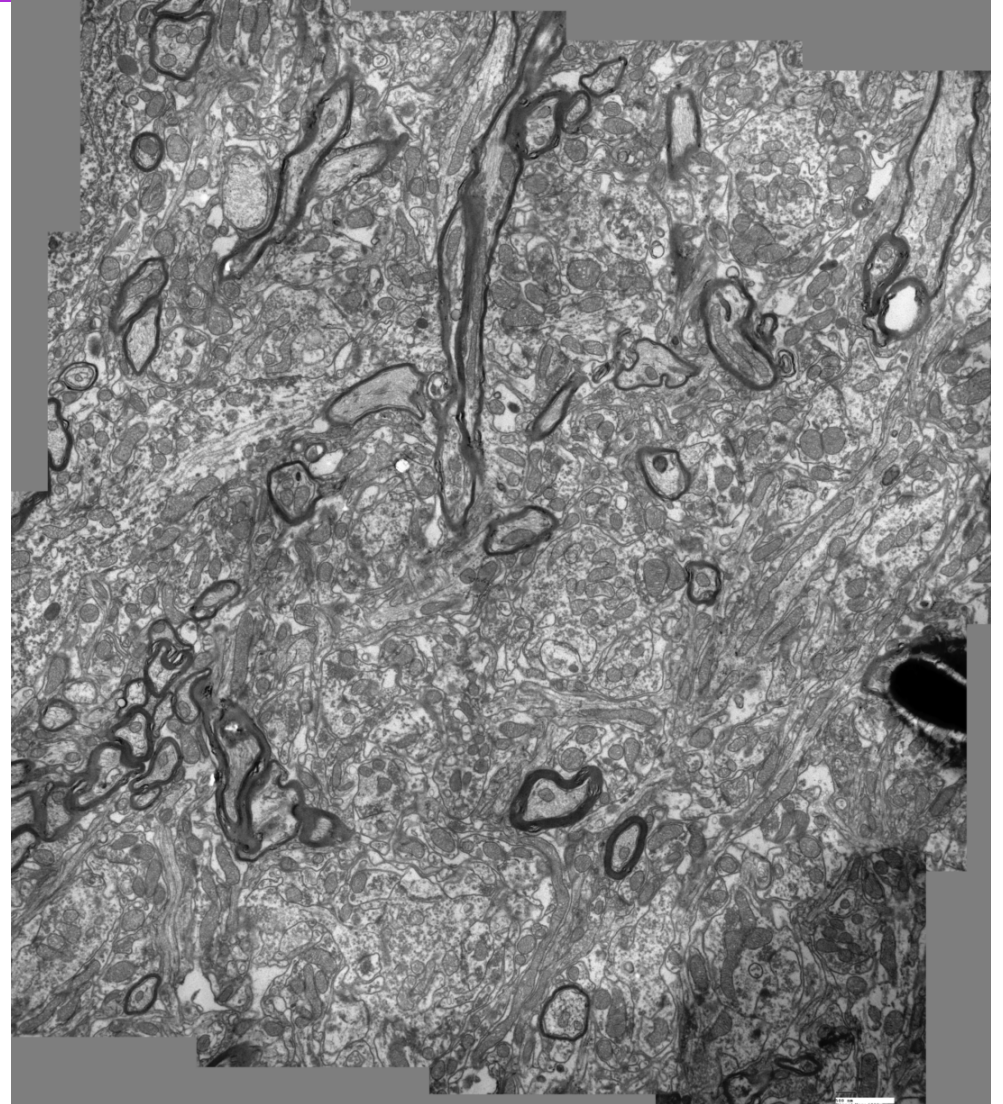
# Objective

Accelerated and improved computational algorithms forming 3D volumes to assess neural ultrastructure in large transmission electron microscopy (TEM) images.

**Image Registration:** finding the transformation that aligns images into one frame of reference.

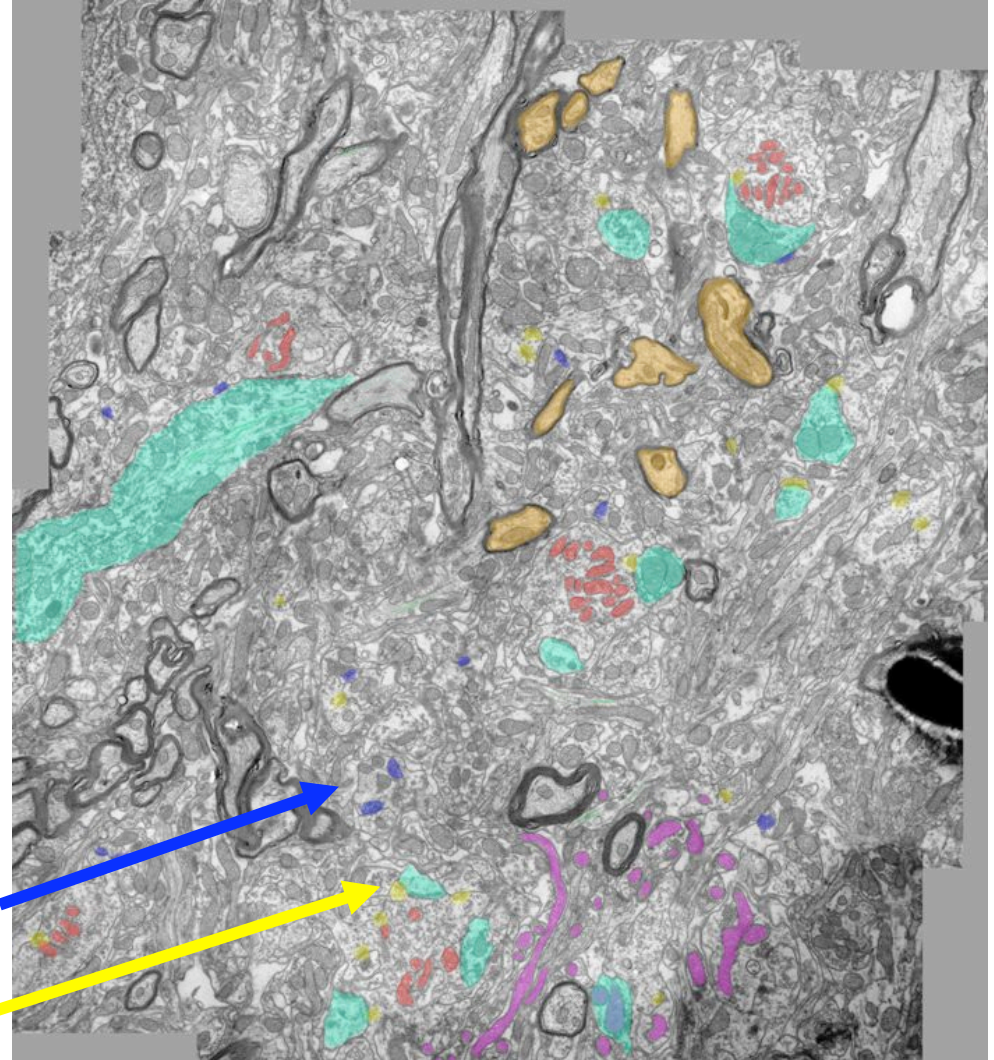
# Manual Expert Tracing of Objects

- 4nm x 4nm x 40nm
- Assuming 6 months of 24/7, camera array  
5-8Mp/s → ~400 $\mu$ m cube
- Pixels: 100k x 100k x 10k
- Terabyte image volumes



# Manual Expert Tracing of Objects

- Mapping of objects and their connections.
- Inherently multi-scale processes. Small circuits extend through volumes of many cubics of  $\mu\text{m}$
- Slow! Terabyte-scale volumes
- Inter-expert and intra-expert variability

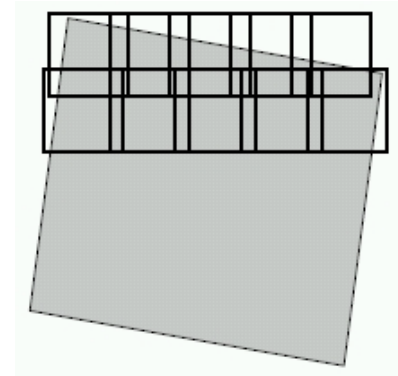
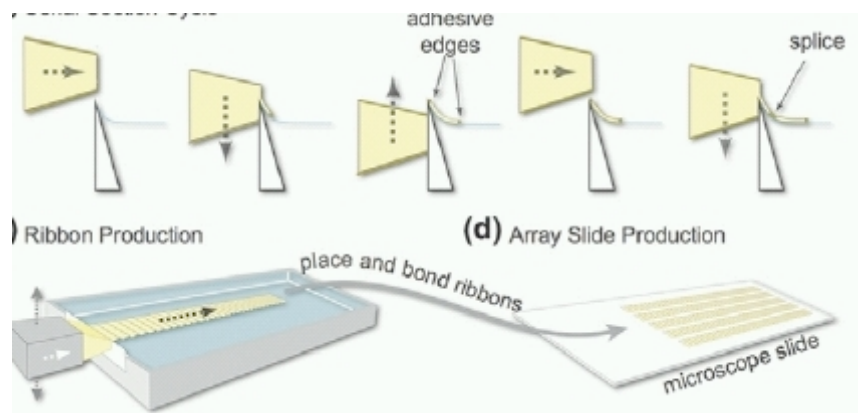


Davi Bock, Neurobiology  
Harvard Medical School

	dendrite		retinogeniculate axon mitochondrion
	myelinated axon		miscellaneous mitochondrion
	excitatory synapse		microtubule
	inhibitory synapse		neurofilament

# Reconstruction of neural circuitry from serial sections of TEM

- Tissue sample is sliced into ultrathin sections with a diamond knife and then each slice is imaged by an electron beam passing through the tissue.
- Building volumes requires to precisely mosaic distorted image tiles and register distorted mosaics.



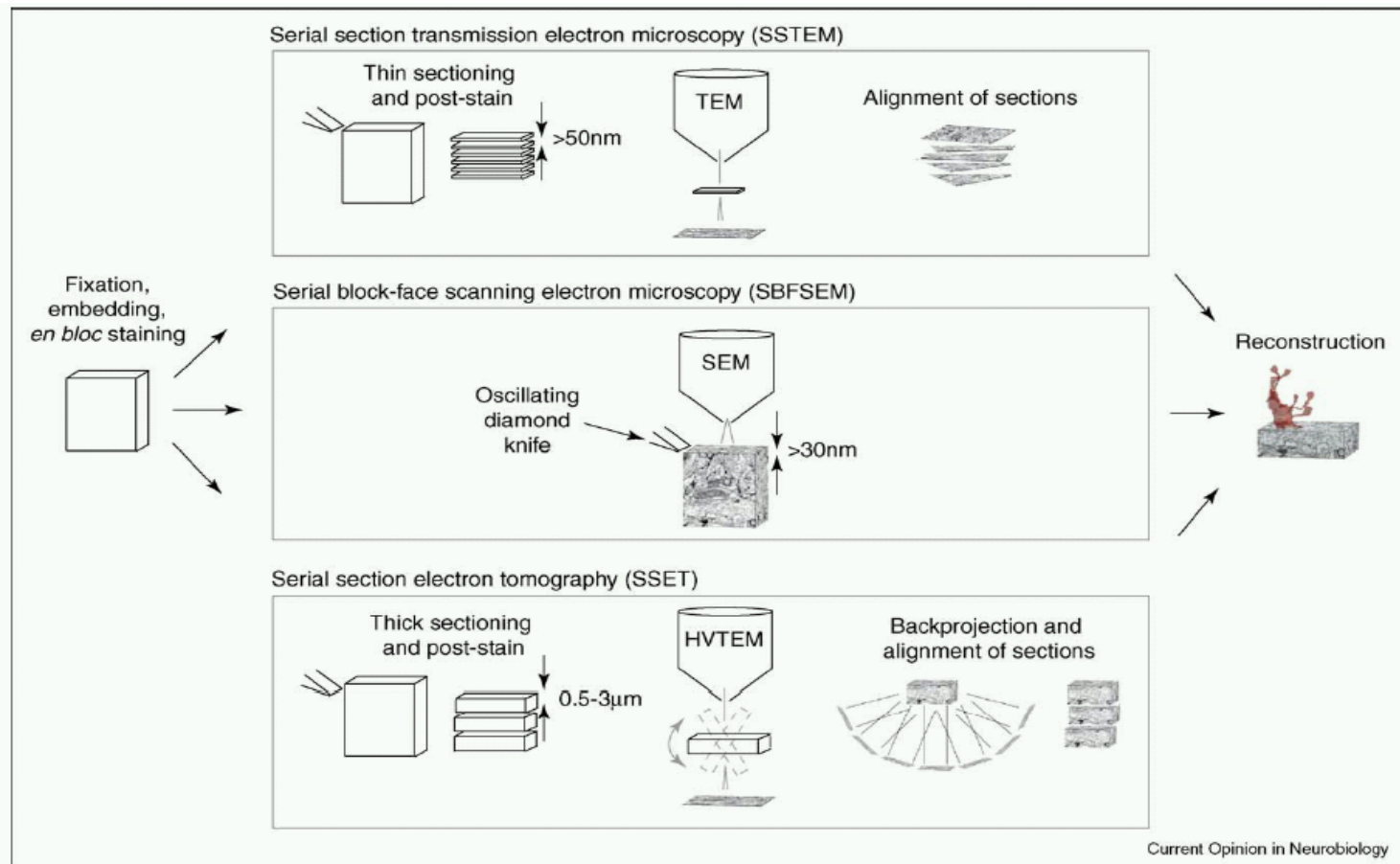
Smith, S. J. (2007). "Circuit reconstruction tools today". *Curr Opin Neurobiol.*

# Main Types of EM Imaging Techniques

<b>Differences</b>	<b>ssTEM</b> Serial section transmission Anderson et al., 2009.	<b>SBFSEM</b> Serial block face scanning Denk and Horstmann, 2004
<b>Cutting from tissue blocks</b>	cut prior to imaging	cut away and discarded after imaging
<b>Image acquisition</b>	transparent' samples	surface imaging. "backscattered electrons detected by scanning remaining block.
<b>Alignment</b>	-Alignment needed	+No alignment
<b>Resolution</b>	+in-section 1-5 nm, high SNR Slice thickness ~50 nm	-in-section 20-30 nm per pixel Thickness 25 nm

\***SSET/ EMT** Similar resolution, low SNR  
artifacts due to limited acquisition angles

# Main Types of EM Imaging Techniques



A schematic diagram of the steps involved in the acquisition of tissue volumes using SSTEM, SBFSEM and SSET. The main differences between these techniques are how sections are cut from embedded tissue blocks, the process of image acquisition and the subsequent alignment of images. Sections are cut prior to imaging in SSTEM and SSET, but after imaging in SBFSEM. Transmission electron microscopy (TEM) and high-voltage transmission electron microscopy (HVTEM) are imaging techniques that require 'transparent' samples; scanning electron microscopy (SEM), however, is a surface imaging technique. Image stacks collected in the SBFSEM need no further alignment prior to reconstruction. See text for a more detailed description of each technique.

K.L. Briggman and W. Denk, Curr. Opinion in Neurobiology 2006

# Significance

- TEM which provides resolutions on the order of a nanometer, is the **primary tool** for resolving the 3D network structure and connectivity of neurons (e.g. required resolution is  $\sim 2$  nm for synapses ).
- Mapping neural circuits can advance understanding of **brain structure and function**.
- Insight into abnormal brain connectivity and **disorders** such as autism and epilepsy.

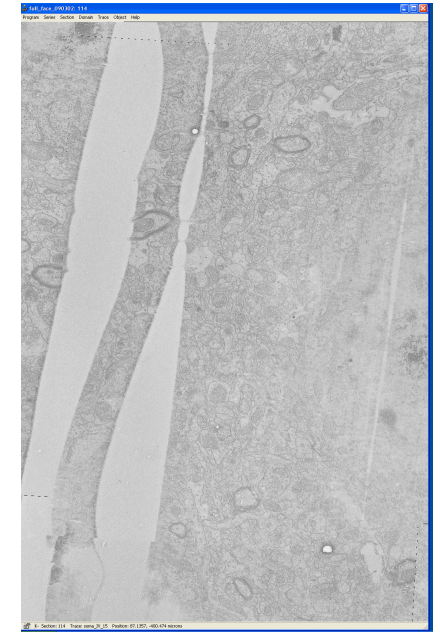
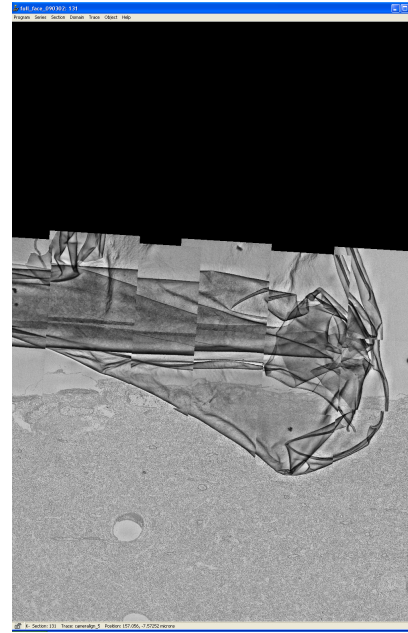
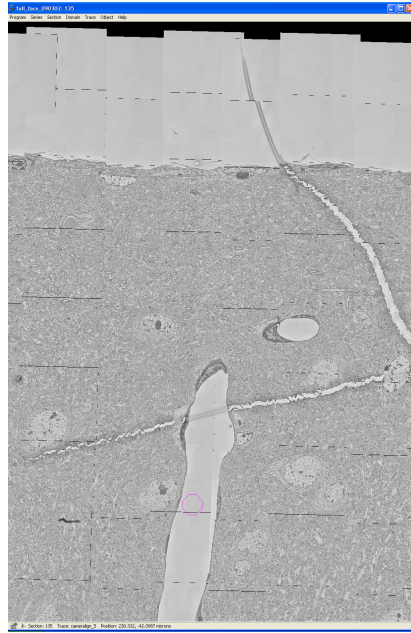
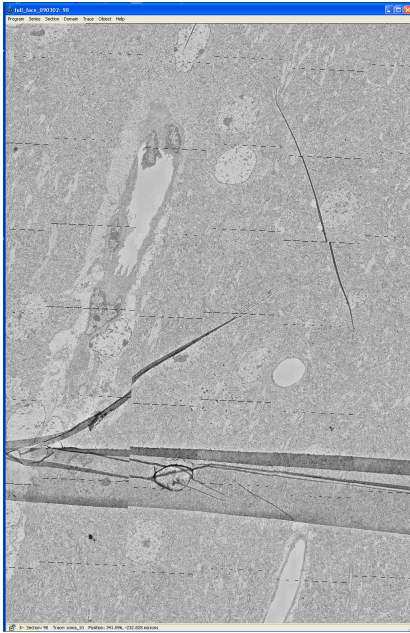
**TEM acquisition is progressing efficiently, the computational tools are the bottleneck!**

# Challenges

- High resolution and large size of the images.
- Large amount of details for relevant features
  - Tracing vulnerable structures across large volumes.
  - Neuronal diversity is high.
- Deformation induced by both the acquisition process and the intrinsic deformation of slices
  - physically separate objects.
  - distortions during handling.
  - distortions by electron beam exposure.
  - Artifact: folds, burns, tears.

**Prevents using classical approaches developed for conventional imaging modalities.**

# Artifacts



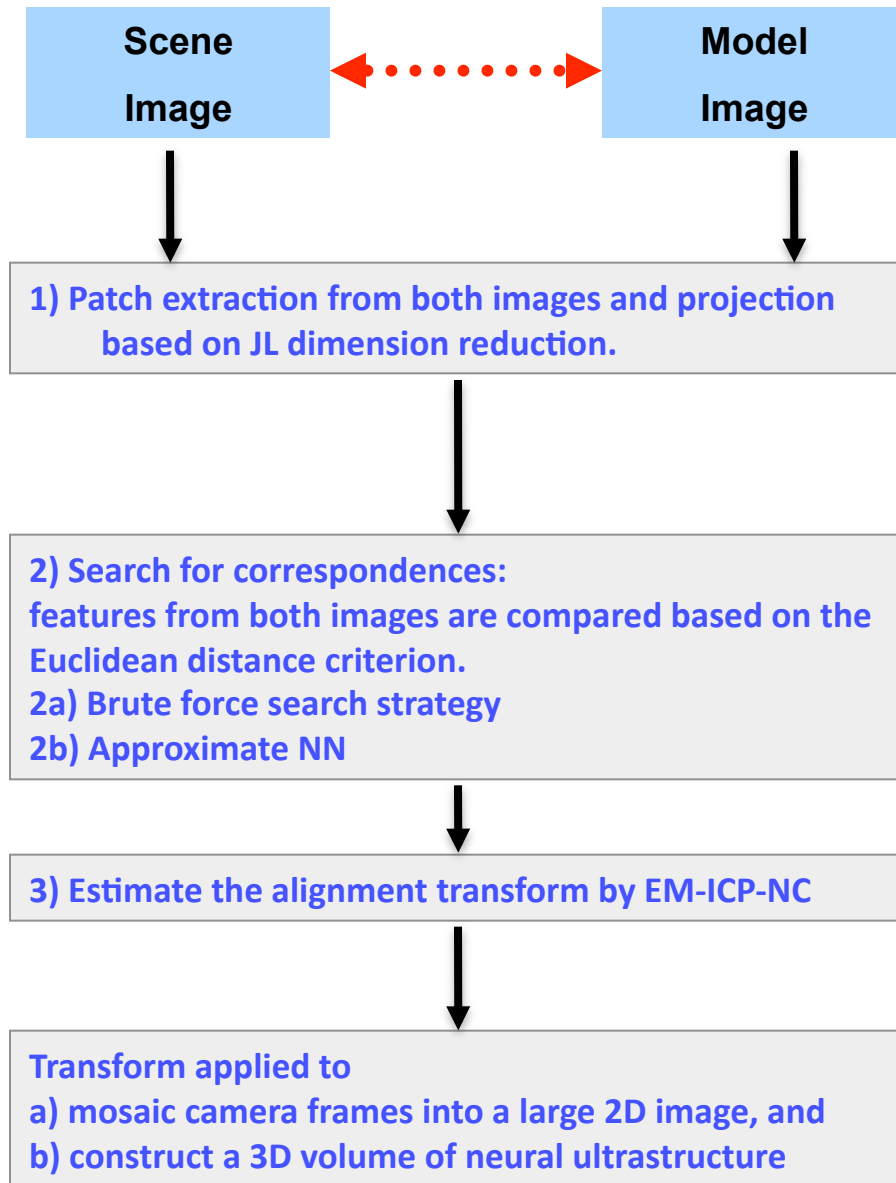
**Folds and Splits**

**Film: holes, coming in,  
excess support film**

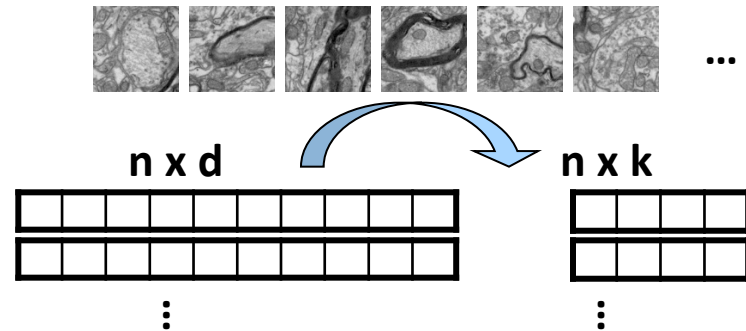
# Background: Registration Algorithms

- Can be classified into:
  - **Voxel intensities statistics**: utilize an information theoretic objective function and an optimizer that finds a local optimum of the objective function.
  - **Feature-based**: identify features to be aligned and an optimal transformation that brings them into alignment.
- Algorithms for EM images:
  - **Ourselin, S. et al. (IVC 2000)**: block matching to estimate a global rigid transformation.
  - **Anderson et al. (Plos Biology 2009)**: A complete framework mosaicking, reconstruction and visualization (Fourier shift property and landmark based approach).
  - **Dauguet, J., et al. (MICCAI 2007)**: finite support properties of the cubic B-splines, where the initial estimate for the affine registration was based Ourselin et al.

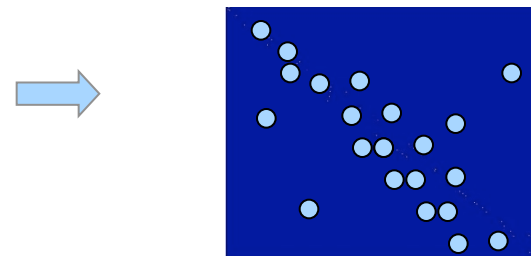
# Schematic Outline of Alignment Process



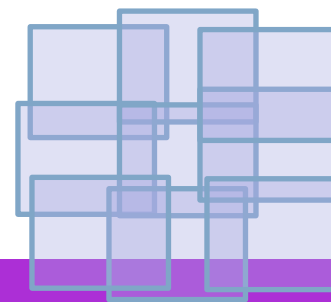
Input: TEM tiles or 2D Mosaic Images



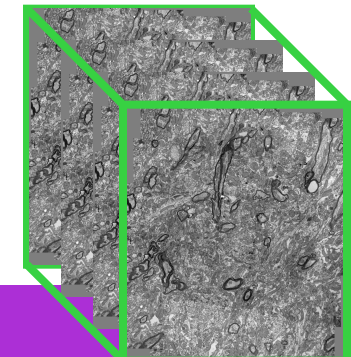
Correspondence matrix



Mosaic Images



Volume reconstruction



# Optimality of Template Matching

Template matching by correlation is the optimal linear operation for detecting a deterministic signal in the presence of additive white noise.

Brunelli, R., and T. Poggio. 1997. Pattern Recognition.

consider a signal:

$$s(x) = \phi(x - x_0) + \lambda(x)$$

template at  $x_0$ , with  
power spectrum  $\Phi(\omega)$

additive  
white noise

filter response for signal detection:

$$z(x) = s(x) * h(x) = \phi(x - x_0) * h(x) + \lambda(x) * h(x) = z_\phi(x) + z_\lambda(x)$$

$$SNR = \frac{|z_\phi(x_0)|^2}{E\{z_\lambda^2(x_0)\}}$$

SNR definition: filter response at  $x_0$  to the variance of the noise  
(assumed to be wide-sense stationary with zero average)

Based on the Schwartz inequality the filter that maximizes the SNR is

$$H(\omega) = \alpha \Phi(\omega) e^{-i\omega x_0}$$

the optimal filter in the spatial domain

$$h(x) = \alpha \phi(x_0 - x)$$

template rotated by 180° and  
translated to  $x_0$

Correlation with the template leads to optimal detection as it maximizes the SNR.

# Template matching by Correlation

- Normalized Correlation (NC) similarity measure is extensively used.

$$NC(p_s, p_m) = \frac{\text{cov}(p_s, p_m)}{\sqrt{\text{var}(p_s)\text{var}(p_m)}}$$

- NC is invariant to linear intensity transformation and for small corresponding image patches in two successive slices, the intensities are locally related by some linear intensity transformation.

**NC is equivalent to a squared Euclidean distance meets the requirements of the JL Lemma.**

# Equivalence of NC and Euclidean distance when the patches are set to be zero mean and unit length.

rately, one can try to detect it with an operator called a *template*. This template is, in effect, a subimage that looks just like the image of the object. A similarity measure is computed which reflects how well the image data match the template for each possible template location. The point of maximal match can be selected as the location of the feature. Figure 3.3 shows an industrial image and a relevant template.

## Correlation

One standard similarity measure between a function  $f(\mathbf{x})$  and a template  $t(\mathbf{x})$  is the Euclidean distance  $d(\mathbf{y})$  squared, given by

$$d(\mathbf{y})^2 = \sum_{\mathbf{x}} [f(\mathbf{x}) - t(\mathbf{x} - \mathbf{y})]^2 \quad (3.1)$$

By  $\sum_{\mathbf{x}}$  we mean  $\sum_{x=-M}^M \sum_{y=-N}^N$ , for some  $M, N$  which define the size of the template extent. If the image at point  $\mathbf{y}$  is an exact match, then  $d(\mathbf{y}) = 0$ ; otherwise,  $d(\mathbf{y}) > 0$ . Expanding the expression for  $d^2$ , we can see that

$$d^2(\mathbf{y}) = \sum_{\mathbf{x}} [f^2(\mathbf{x}) - 2f(\mathbf{x})t(\mathbf{x} - \mathbf{y}) + t^2(\mathbf{x} - \mathbf{y})] \quad (3.2)$$

Notice that  $\sum_{\mathbf{x}} t^2(\mathbf{x} - \mathbf{y})$  is a constant term and can be neglected. When  $\sum_{\mathbf{x}} f^2(\mathbf{x})$  is approximately constant it too can be discounted, leaving what is called the *cross correlation* between  $f$  and  $t$ .

$$R_{ft}(\mathbf{y}) = \sum_{\mathbf{x}} f(\mathbf{x})t(\mathbf{x} - \mathbf{y}) \quad (3.3)$$

This is maximized when the portion of the image “under”  $t$  is identical to  $t$ .

Ballard D.H. and Brown C.M., (1982)

# Contribution

1. A novel efficient search strategy that enabled us to dramatically accelerate feature based registration.
2. A novel algorithm (EM-ICP-NC) for robust estimation of alignment transformation once the exact/probabilistic correspondence is determined.
3. Evaluation of randomized projection for dimensionality reduction in the registration.
4. Results demonstrating alignment of TEM images of neural ultrastructure with increased accuracy and efficiency.

# Outline

- I Background
  - Electron Microscopy
  - Related work
- **II Methods**
  - **Dimensionality Reduction**
  - Nearest Neighbor Search
  - Transformation Estimation (EM-ICP-NC)
- III Experiments and Results
- IV Summary

# Johnson-Lindenstrauss (JL) Lemma

Any set of  $n$  points in  $d$ -dimensional Euclidean space can be embedded into dimension  $k = O\left(\log \frac{n}{\epsilon^2}\right)$  is logarithmic in  $n$  and independent of  $d$ , while maintaining pairwise distances with a distortion of at most  $\epsilon$ .

Johnson, W.B. Lindenstrauss, J. (1984) "Extensions of Lipschitz mappings into a Hilbert space", *Contemp Math*, 26: 189-206.

# Notations for Dimensionality reduction

- **n** - the size of the data set
- **d** - the dimension of Euclidean space
- **k** - the reduced dimension
- **$\epsilon$**  - the distortion rate
- **R** - random matrix projecting the points from  $\mathbb{R}^d$  to  $\mathbb{R}^k$ .

# Achlioptas (2003)

Let  $P$  be a set of  $n$  point in  $R^d$ , represented as an  $n \times d$  matrix  $A$ .

Then given  $\varepsilon, \beta > 0$  let  $k_0 = \frac{4 + 2\beta}{\varepsilon^2/2 - \varepsilon^2/2} \log n$

For integer  $k \geq k_0$ , let  $R$  be a  $d \times k$  random matrix with  $R(i, j) = r_{ij}$ ;

Where the independent random variable  $r_{ij}$  are from either one of the following two distributions:

$$r_{ij} = \begin{cases} 1 & \text{with probability } 1/2 \\ -1 & \text{with probability } 1/2 \end{cases}$$

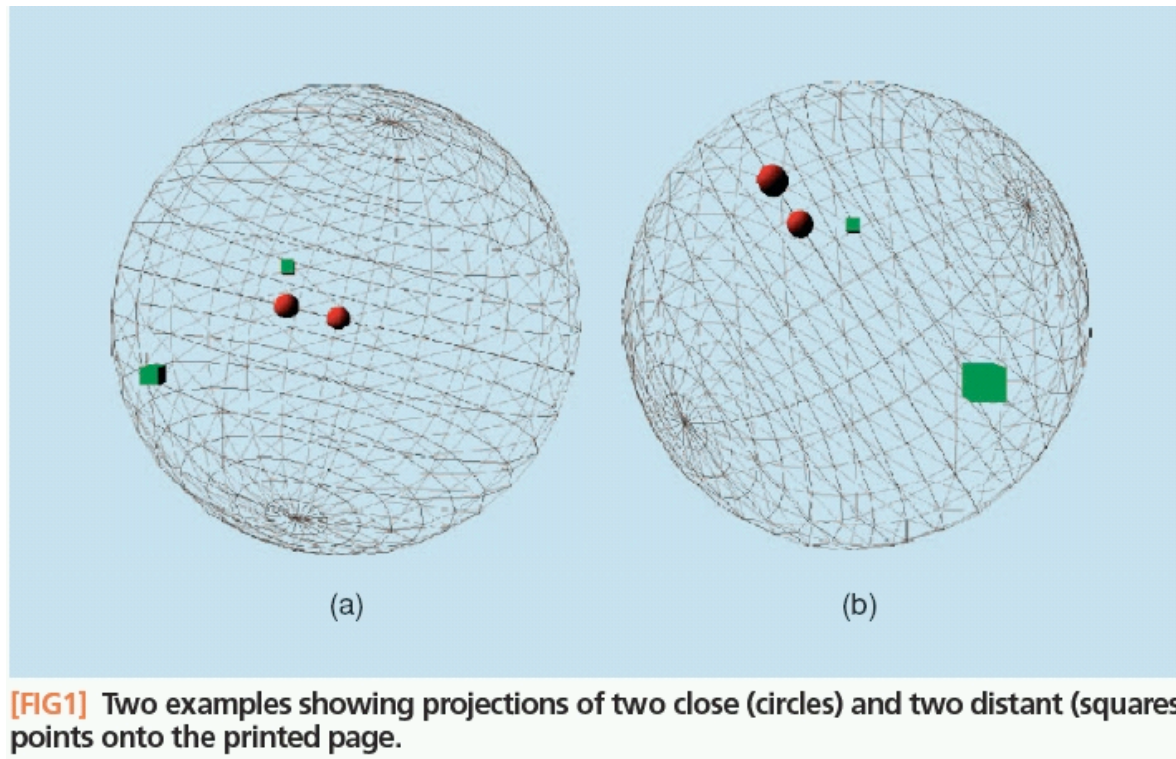
$$r_{ij} = \sqrt{3} \begin{cases} 1 & \text{with probability } 1/6 \\ 0 & \text{with probability } 2/3 \\ -1 & \text{with probability } 1/6 \end{cases}$$

Let  $E = \frac{1}{\sqrt{k}} AR$  and let  $f : R^d \rightarrow R^k$  map the  $i^{\text{th}}$  row of  $A$  to the  $i^{\text{th}}$  row of  $E$

Then with probability of at least  $1 - n^{-\beta}$ , for all  $u, v \in P$ :

$$(1 - \varepsilon) \|u - v\|^2 \leq \|f(u) - f(v)\|^2 \leq (1 + \varepsilon) \|u - v\|^2$$

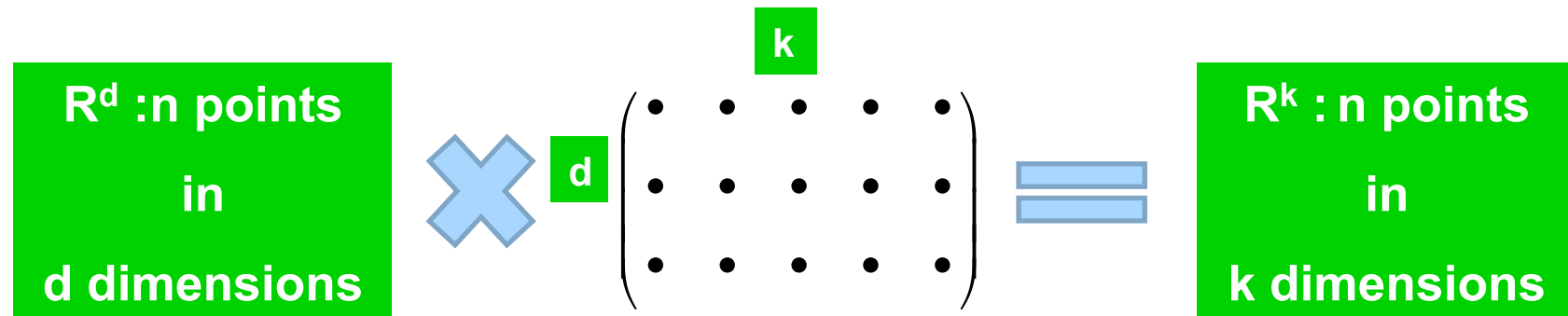
# Some Intuition/ Illustrative Example



Two points that are close together on the sphere are also close together when the sphere is projected onto the 2D page. This is true no matter how we rotate the sphere.

From: Slaney and Casey 2008

# Random Projections in Practice



- Naïve JL solution: dense random matrix
  - $k < d$ ,
  - $O(dk)$  per data feature
- Open Questions:
  - How to selection the dimension  $k$ ?
  - Faster projection schemes  $O(d)$  using sparse matrices

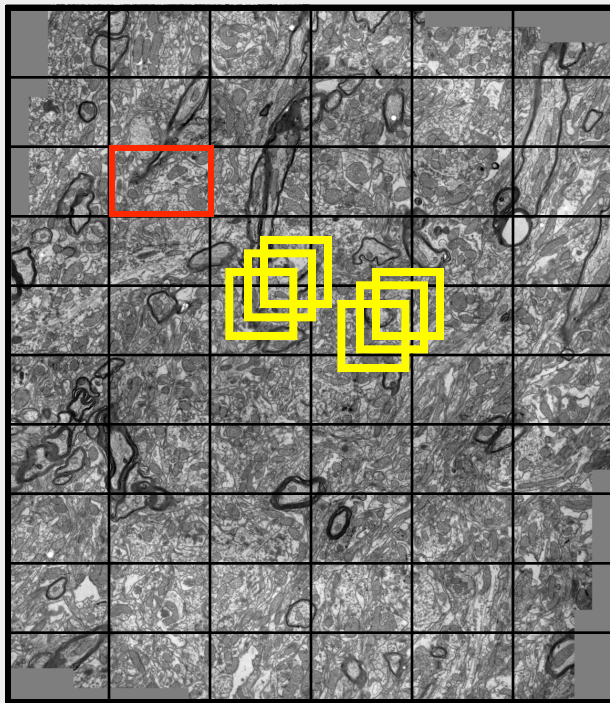
E. Liberty 2009

# Outline

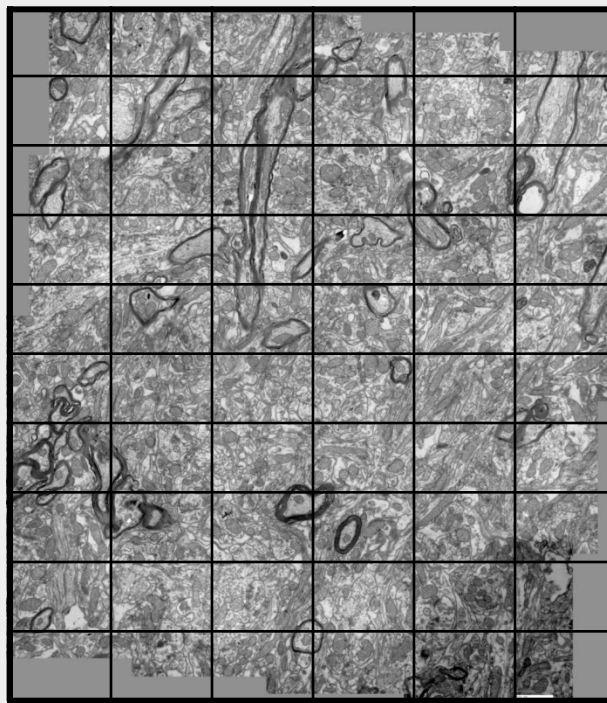
- I Background
  - Electron Microscopy
  - Related work
- **II Methods**
  - Dimensionality Reduction
  - **Nearest Neighbor Search**
  - Transformation Estimation (EM-ICP-NC)
- III Experiments and Results
- IV Summary

# Search For Correspondences

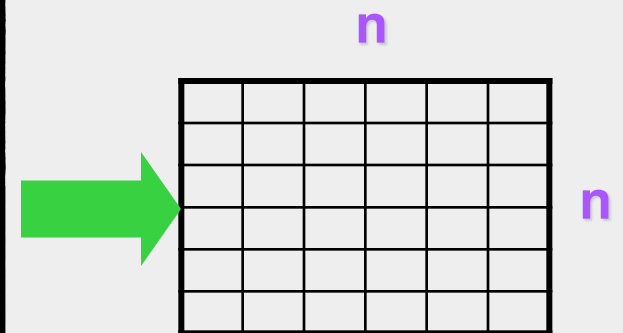
Moving Scene (n)



Fixed Model (n)



Similarity Matrix

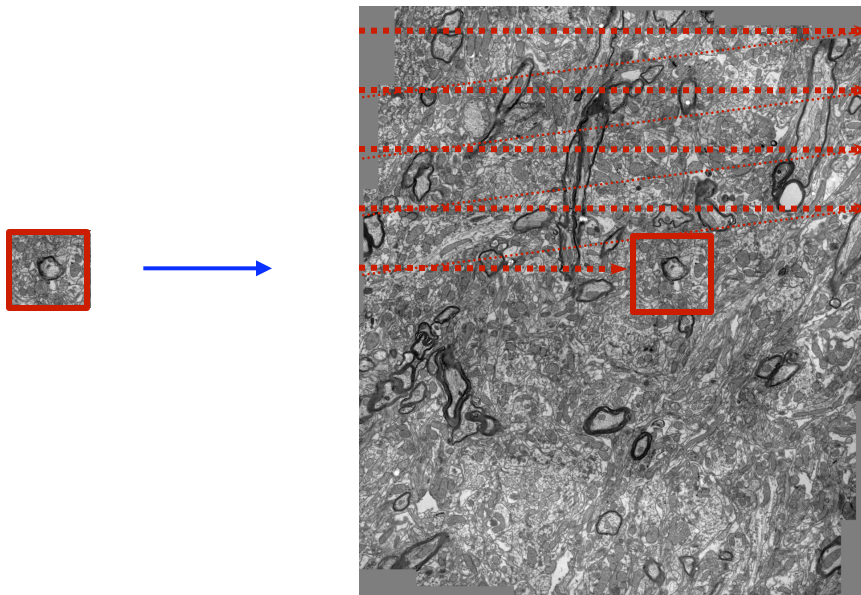


# Nearest Neighbor (NN) Search

Given a set  $\mathbf{P}$  of data points in  $\mathbb{R}^d$ , and query point  $\mathbf{q}$ :

**NN:** returns a point  $\mathbf{p}$  in  $\mathbf{P}$  minimizing  $\|\mathbf{p}-\mathbf{q}\|$ .

**Brute force Search:** Calculate the distance from  $\mathbf{q}$  to every  $\mathbf{p}$  and choose the point with minimal distance.



**Slow!**  
 **$O(dn)$**

# Curse of dimensionality

- **Current solutions for solving the NN problem require either space or query time exponential in dimensionality  $d$ .**
- When dealing with a large dimensions, in practice the solutions often provide little improvement over the naïve algorithm.
- The failure of these search algorithms which are efficient in low-dimensional spaces to succeed in high-dimensions has been called the **`curse of dimensionality`**: **Exponential dependence of the algorithm on the dimension of the input.**

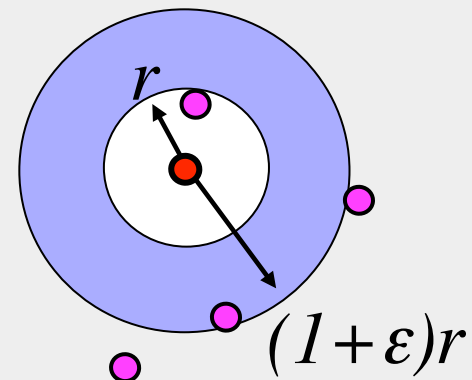
Andoni and Indyk 2006

# Approximate Nearest Neighbor (ANN)

- **c-ANN**: given a  $c > 0$ , returns a point  $p \in P$  s.t.  $\|p - q\|$  is at most  $c = (1 + \epsilon)$  factor larger from the distance of the nearest point  $p \in P$  from  $q$ .

Query time: **Fast!**  $O(dn^{\rho(c)})$

space  $O(dn^{1+\rho(c)})$  where  $\rho(c) = 1/c^2 + O(1)$ .



- Recently several probabilistic algorithms have been proposed for ANN search. The algorithms yield **sublinear complexity** in the size of the data.
- This approach results in efficient algorithms which are based on data structures such as **locality sensitive hashing (LSH)** and **tree based search**.

Indyk, P. Motwani, R. (1998)

# Outline

- I Background
  - Electron Microscopy
  - Related work
- **II Methods**
  - Dimensionality Reduction
  - Nearest Neighbor Search
  - **Transformation Estimation (EM-ICP-NC)**
- III Experiments and Results
- V Summary

# EM-ICP-NC Notation

- $\mathbf{s}_i$ : points of the scene patch set  $S \in R^2$
- $\mathbf{m}_j$ : points of the model patch set  $M \in R^2$
- $n_s, n_m$ : # of points respectively
- $\mathbf{T}$ : transformation (scene  $\rightarrow$  model)
- $\mathbf{A} \in R^{n_s \times n_m}$  correspondence matrix (for each scene point indication the matching point).

P.J. Besl and N.D. McKay, IEEE PAMI, 14(2):239–256, 1992.

S. Granger and X. Pennec, Miccai 2001 eccv 2002

# Probability Distribution of Correspondences

- The probability of  $\mathbf{s}_i$  to correspond to  $\mathbf{m}_j$  can be modeled by a Gaussian distribution.
- In the case of homogeneous isotropic Gaussian noise, where  $\sigma$  represents the noise in the measurement  $\mathbf{s}_i$ .

$$p(\mathbf{s}_i | \mathbf{m}_j, \mathbf{T}) = \exp\left(-\frac{\|\mathbf{T} \cdot \mathbf{s}_i - \mathbf{m}_j\|^2}{2\sigma^2}\right)$$

# EM-ICP-NC

- The idea is to maximize the log-likelihood of the data distribution

$$\log p(\mathbf{S}, \mathbf{A} \mid \mathbf{M}, \mathbf{T})$$

- The correspondences are unknown hidden random variables

$$\mathbf{A} \in \mathcal{R}^{n_s \times n_m}$$

# EM-ICP framework

start

Initialization (T)

E-Step : Inference (A)

Compute the probability for A, given the current estimate of T parameters.

iterate

M-Step: Reparameterize (T)

Estimate T using the probability of A

[Dempster et al. 1977]

# EM-ICP

- Represent the correspondence estimation as an indicator variable  $A_{ij} = 1$  iff  $s_i$  matches  $m_j$   
 $A_{ij} = 0$  otherwise.

- The joint probability of  $s_i$  and  $A_{ij}$  is the product

$$p(s_i, A_{ij} = 1 \mid M, T) = \pi_{ij} p(s_i \mid m_j, T)$$

- The joint likelihood of all the  $S, A$

$$p(S, A \mid M, T) = \prod_{ij} \left( \pi_{ij} p(s_i \mid m_j, T) \right)^{A_{ij}}$$

# E-Step

- The **prior** is based on the NC patch measure defined, which encodes knowledge on the structure of the objects.

$$\pi_{ij} = \frac{NC(p_i, p_j)}{\sum_k NC(p_i, p_k)}$$

- T is fixed and the probability of the matches A are estimated.

$$p(\mathbf{A} \mid \mathbf{S}, \mathbf{M}, \mathbf{T}) = \frac{p(\mathbf{S}, \mathbf{A} \mid \mathbf{M}, \mathbf{T})}{p(\mathbf{S} \mid \mathbf{M}, \mathbf{T})} = \prod_{ij} \left( \frac{\pi_{ij} p(\mathbf{s}_i \mid \mathbf{m}_j, \mathbf{T})}{\sum_k \pi_{ik} p(\mathbf{s}_i \mid \mathbf{m}_k, \mathbf{T})} \right)^{A_{ij}}$$

- Compute the expectation:

$$E(A_{ij}) = \frac{\pi_{ij} \exp\left(-\frac{\|\mathbf{T} \cdot \mathbf{s}_i - \mathbf{m}_j\|^2}{2\sigma^2}\right)}{\sum_k \pi_{ik} \exp\left(-\frac{\|\mathbf{T} \cdot \mathbf{s}_i - \mathbf{m}_k\|^2}{2\sigma^2}\right)}$$

# M-step

- The expected value of the complete data log-likelihood is maximized to find the new estimate of  $\mathbf{T}$ :

$$\mathbf{T}^t = \arg \max_{\mathbf{T}} \left( E \left[ \log p(S, A \mid M, \mathbf{T}) \mid S, M, \mathbf{T}^{(t-1)} \right] \right)$$

- We optimize:

$$\begin{aligned} & E \left[ \log \left( \prod_{ij} \left( \pi_{ij} p(\mathbf{s}_i \mid \mathbf{m}_j, \mathbf{T}) \right)^{A_{ij}} \right) \mid S, M, \mathbf{T}^{(t-1)} \right] \\ &= \sum_i \sum_j E(A_{ij}) \log \left( \pi_{ij} p(\mathbf{s}_i \mid \mathbf{m}_j, \mathbf{T}) \right) \end{aligned}$$

# M-step

- Updated transform  $T$  is given by:

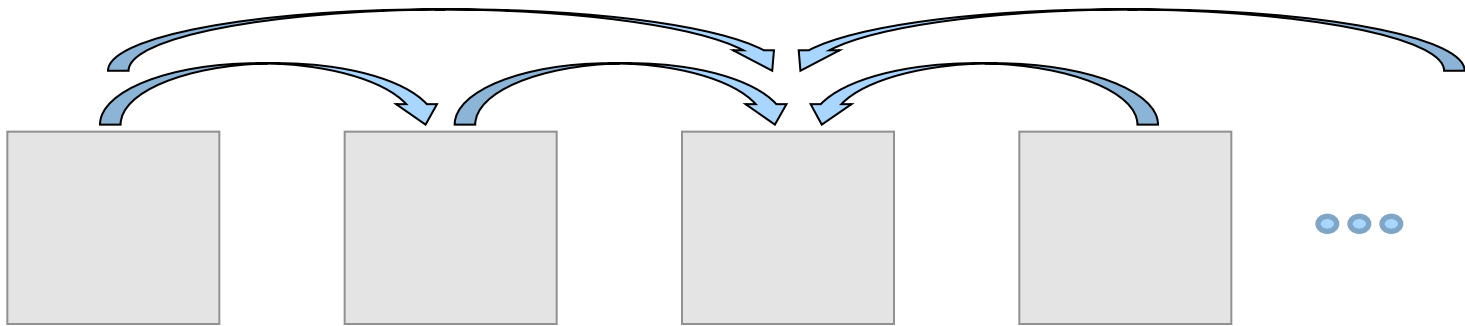
$$T^t = \arg \max_T \sum_i \sum_j \overline{A_{ij}} \frac{-1}{2\sigma^2} \|\mathbf{T} \cdot \mathbf{s}_i - \mathbf{m}_j\|^2$$

# Outline

- I Background
  - Electron Microscopy
  - Related work
- II Methods
  - Dimensionality Reduction
  - Nearest Neighbor Search
  - Transformation Estimation (EM-ICP-NC)
- **III Experiments and Results**
- IV Summary

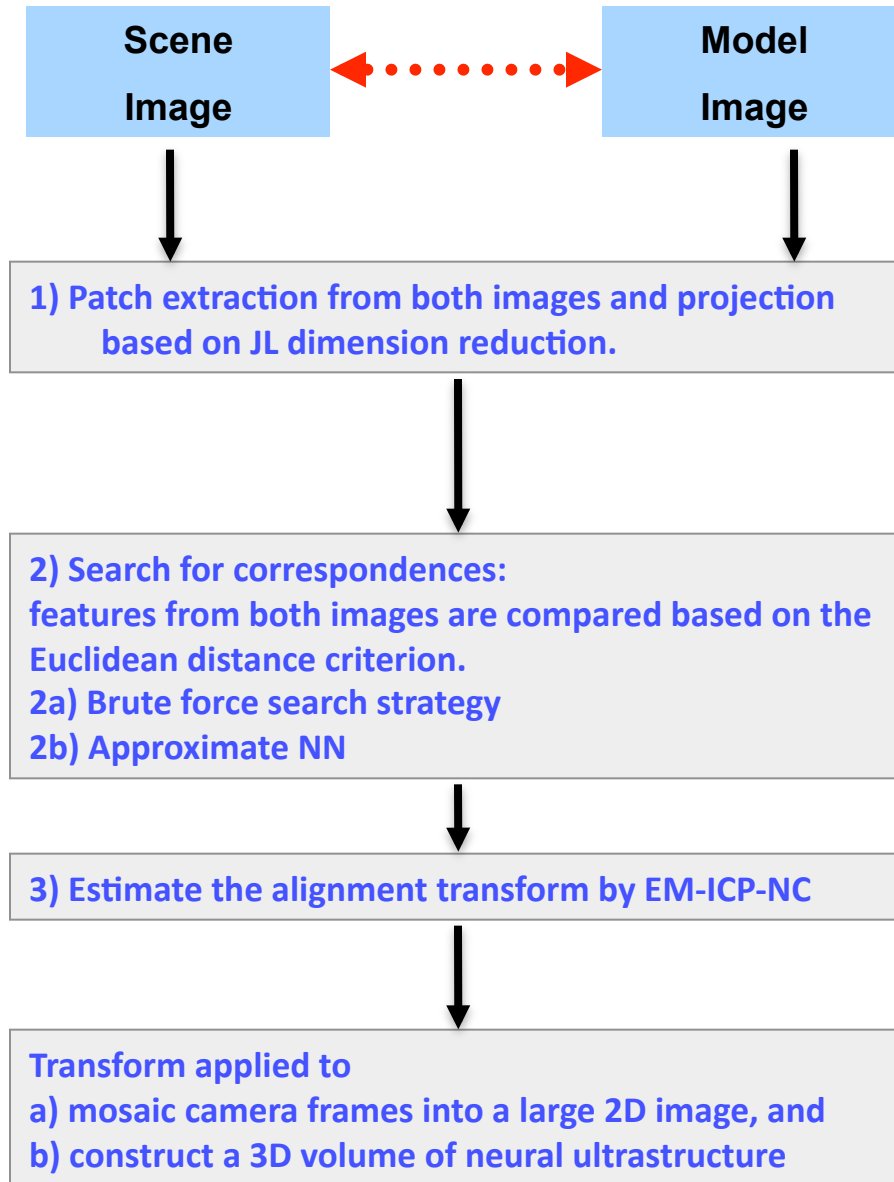
# Volume Reconstruction

Our aim is to find the transformation  $T$  aligning the moving scene  $I_s$  with the fixed model image  $I_M$ .

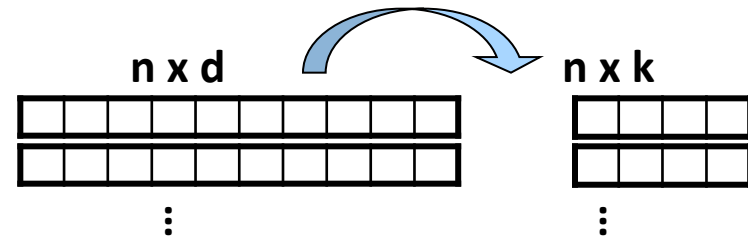
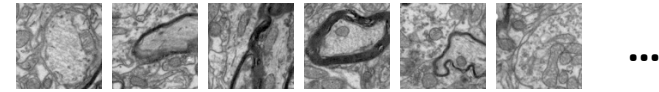


By composing pairwise 2D alignments of consecutive slices while taking as reference the middle of the stack.

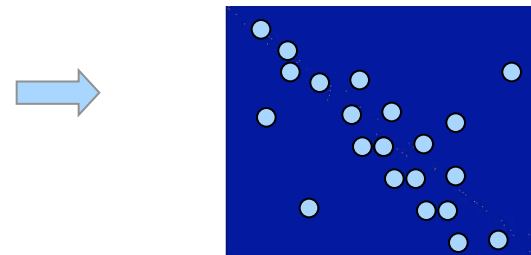
# Schematic Outline of Alignment Process



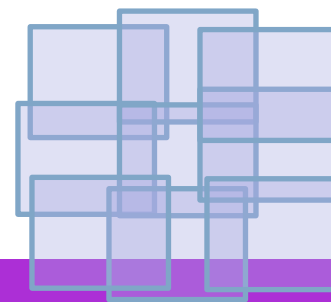
Input: TEM tiles or 2D Mosaic Images



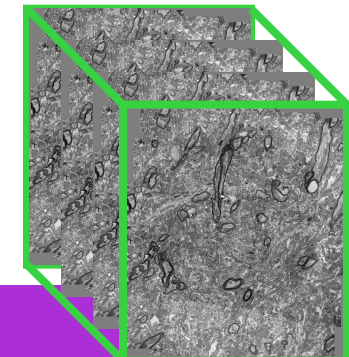
Correspondence matrix



Mosaic Images



Volume reconstruction



# Data

**TEMCA 1.0:** Series of 160 TEM images of the lateral geniculate nucleus of a ferret.

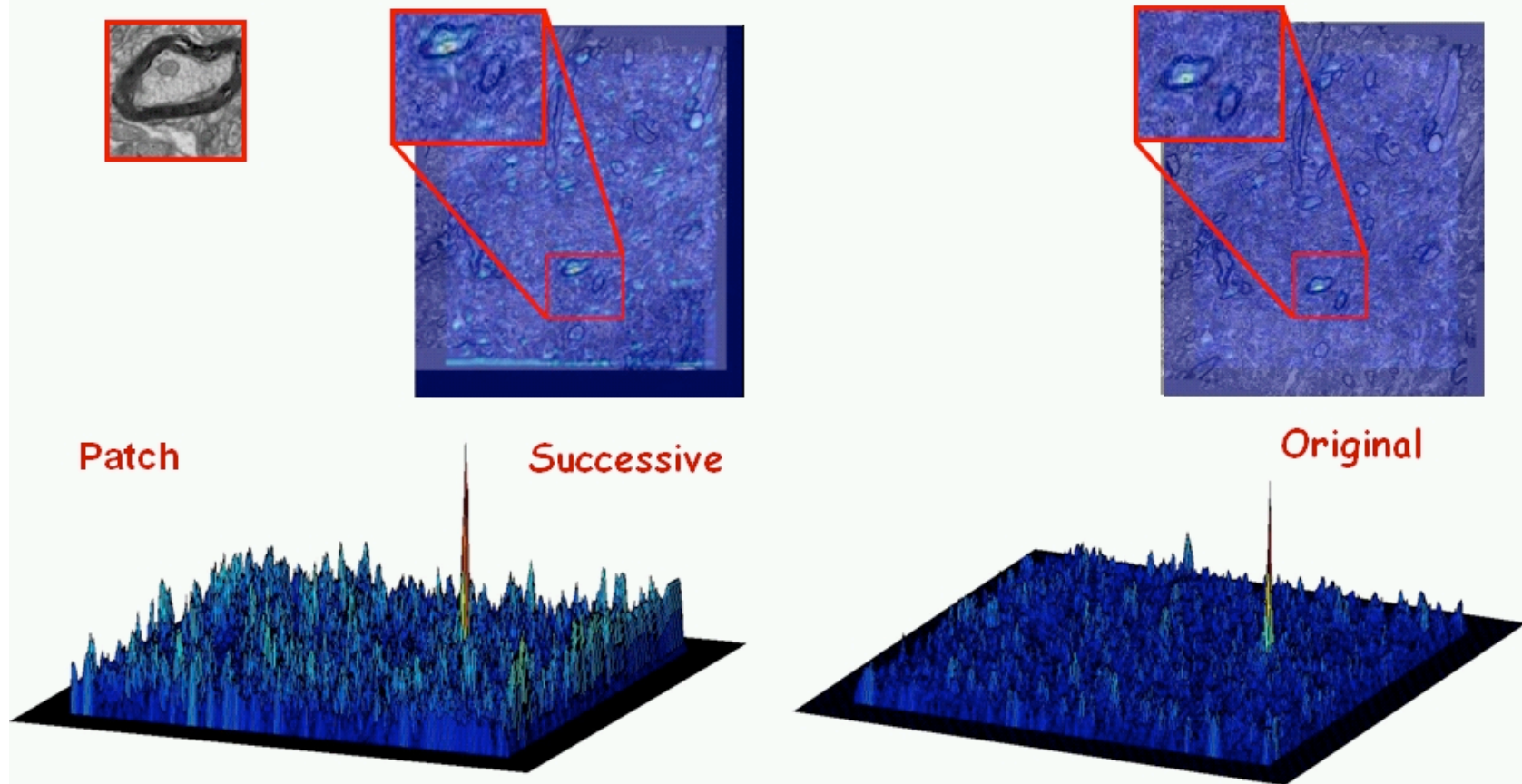
- Each image is about 10,000 × 10,000 pixels
- Pixel resolution of 3nm x 3nm x 60nm.
- Blendmont was used to reconstruct the large field of view image from the 5 × 5 mosaics of smaller images coming from the camera.

**TEMCA 1.5** images of mouse visual cortex from experiment “ms8 6L“. The data consists of 5x5 arrays of tiles from 40 serial sections.

- The pixel size is 3.75nm x 3.75nm and sections are ~45nm thick, 29x53 array spans out to about a 450x850 micron field of view.
- Each image is presented as separate tiles of 5200x5200 pixels;

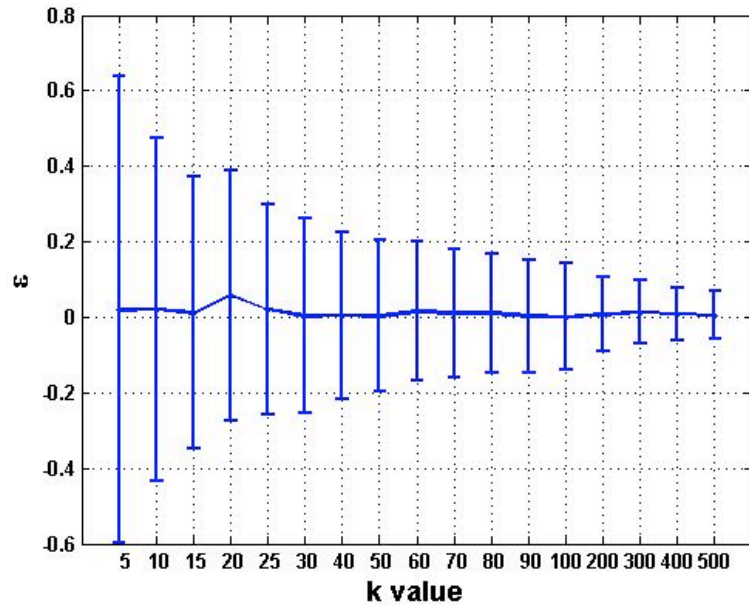
**Blendmont Utility** <http://bio3d.colorado.edu/imod/>

# 1. Effectiveness of Template Matching

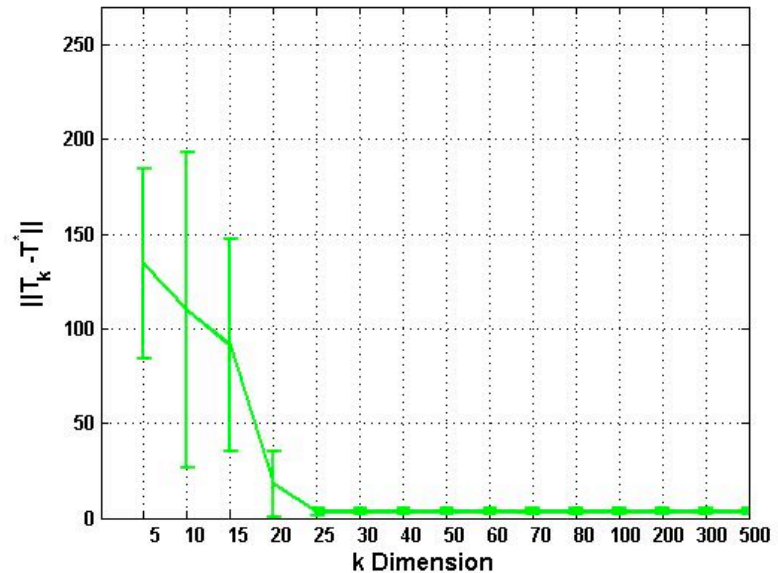


- Correlation maps for patches in original and successive slice were superimposed on images
- The features are a sharp local maxima of the NC.

## 2. Impact of projection to dimension k



(a) Distance Distortion ver. k.  
Decrease in distortion as the projected dimension k increases.



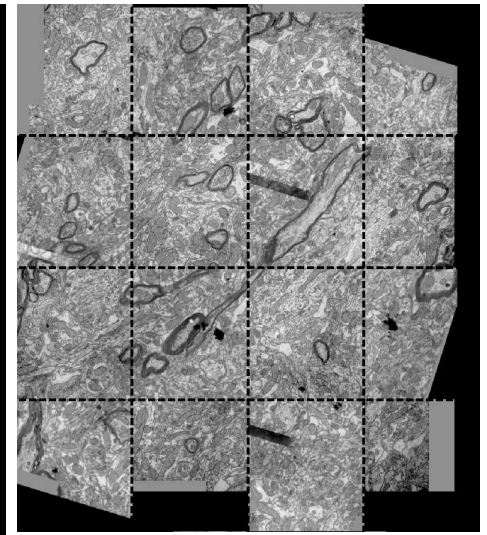
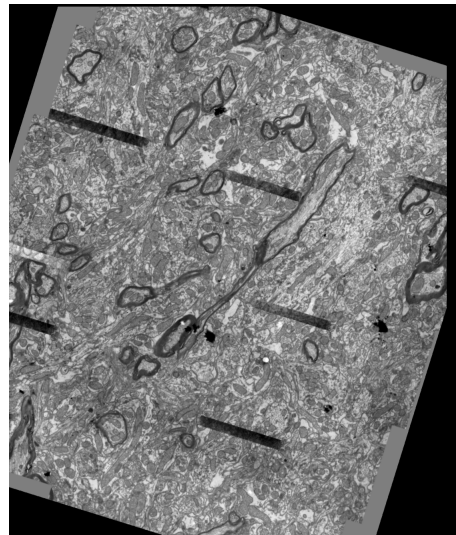
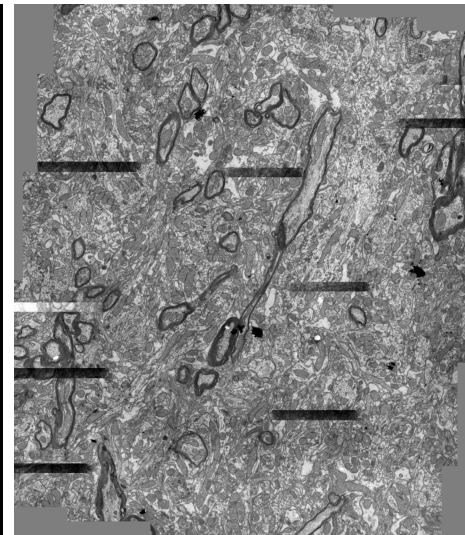
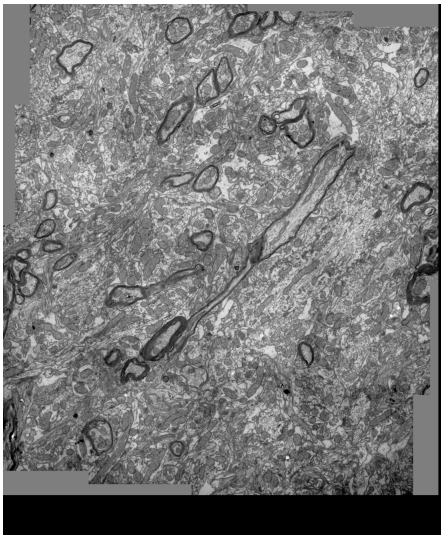
(b) Accuracy of Transformation estimation error vers. k,  
Decreases as k increases.

# 3. Transformation Estimation

<b>Dimension</b>	<b>Scale of 1000x1000</b>	<b>Scale of 5000x5000</b>
<b>K=30 with JL</b>	3.61±2.34	3.1±1.65
<b>d=10000 without JL</b>	3.52±2.66	3.02±1.30

**Comparing the automatic and manual transformations.  
High accuracy is obtained with and without projection.**

# Alignment Visualization



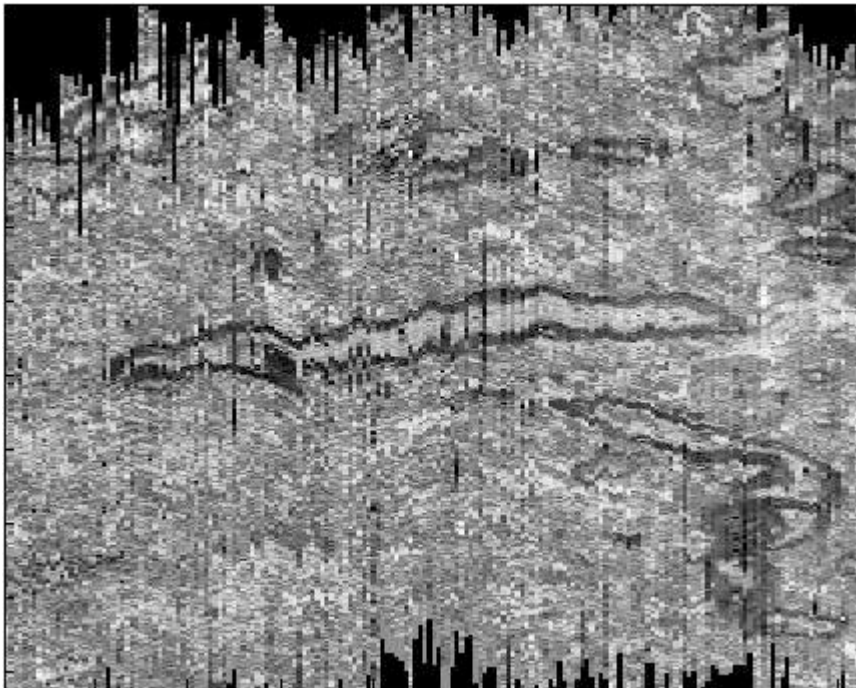
(a) Fixed

(b) Moving before

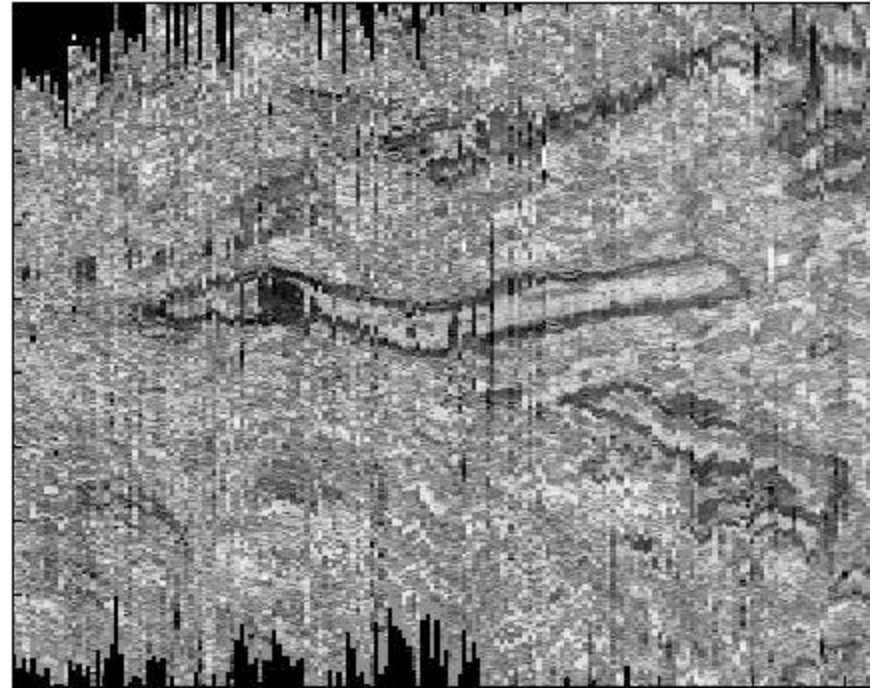
(c) After Alignment

(d) checkerboard composite.

# Orthogonal views of stack reconstruction



**(a) manual**



**(b) automatic k**

## 4. Projection by PCA

- Finds the direction **u** s.t. projecting **n** points in **d** onto **u** gives the largest variance.
- **Formally**: **n** patches of dimension **d**.  $\{x_i\}_{i=1}^n$
- Normalized in advance to have zero mean and unit variance.
- Covariance matrix  $S = \frac{1}{N} \sum_{i=1}^n (x_i - \mu)(x_i - \mu)^T$   $\mu = \frac{1}{n} \sum_i x_i$
- **u** is the eigenvector of **Su=λu**.
- The low dimension space is based on the first **k** eigenvectors ( maximal eigenvalues)

# Projection Schemes

## Randomized

[JL 1984, Achlioptas, Liberty, Ailon, Singer 2008]

Projection s.t the Euclidean distance between features in the low dimensionality projection ~ Euclidean distance between the original features.

Data oblivious

Multiply by the same pre-computed random matrix.

## PCA

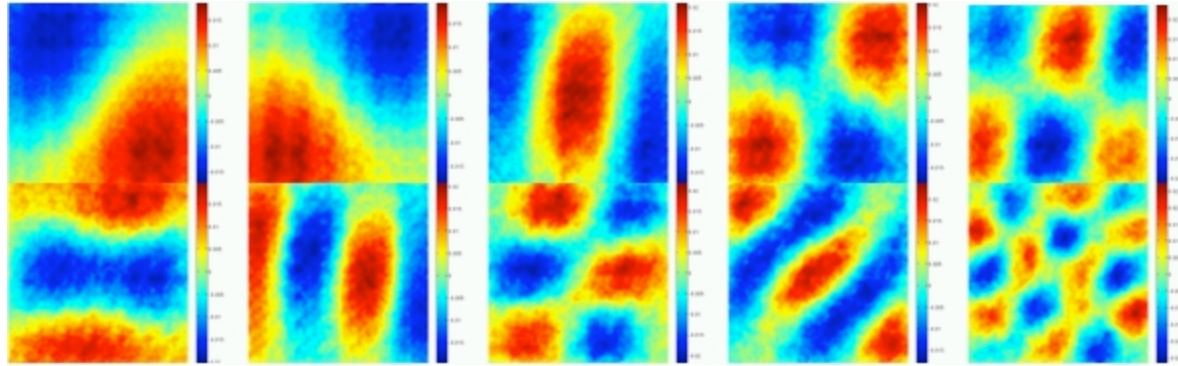
[Turk Pentland 1991, Kirby Sirovich 1990]

Projection on an Eigen-subspace. The Eigen-values correspond to variance and have no guarantees regarding local properties of the resulting projection.

Data aware

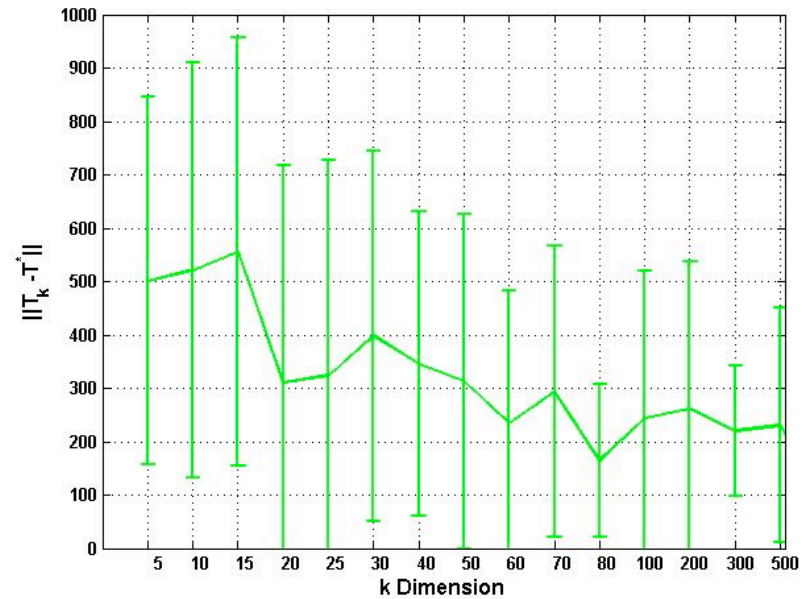
The need to have the same basis function reduces the overall efficiency. An adaptive basis function adds communication cost due to the need to communicate the basis functions.

# Comparison to Projection by PCA



(a) Illustration of Eigenvector images  
k = 1-5 (upper) 6-9, 20 (lower) from left to right.

(b) Transformation error vs. k  
when projecting by PCA.



# 5. Computational complexity

- $T \sim 100$  : # images in the volume.
- $n = M \times M = 10^{10}$  : Size of the images in pixels.
- $d = N \times N = 10^4$  : typical patch/feature dimension .

Brute force Search d:  $O(Tn \cdot nd)$

Brute force Search k:  $O(Tn \cdot n \log n)$

Approximate NN :  $O(Tn \cdot dn^{0.25})$

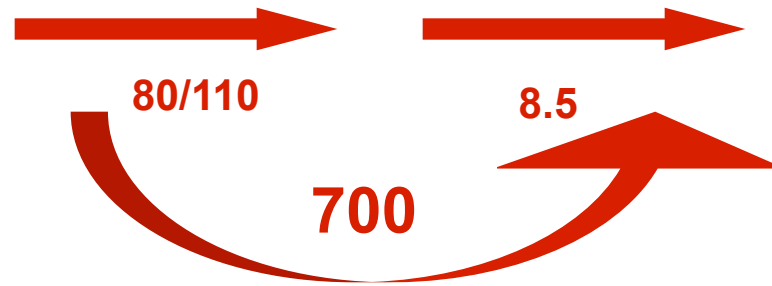
Search time per query in the Accelerated New approach  
by LSH  $O(dn^{1/c^2})$  where for  $c=2$  becomes  $O(dn^{1/4})$

→ **Saving  $O(n^{3/4}) \sim O(10^{7.5})$**

**Potentially more than a million times faster !!!**

# Computational Complexity

Search per n queries	Naive	Naive + JL	Naive + JL + kd-trees	ANN-LSH
Theoretical	$O(n^2d)$	$O(n^2k)$	$O(nkn^{1-\frac{1}{k}})$	$O(ndn^{1/4})$
Practical $n = 42336$	283400sec = 3.3days	3614sec = 60min	420sec = 7min	–
Practical $n = 160000$	$4.4 \times 10^6$ sec $\approx$ 51days <sup>1</sup>	53506sec = 892min	6300sec = 105min	–



Odyssey cluster, FAS Research Computing Group.

# Outline

- I Background
  - Electron Microscopy
  - Related work
- II Methods
  - Dimensionality Reduction
  - Nearest Neighbor Search
  - Transformation Estimation (EM-ICP-NC)
- III Experiments and Results
- **IV Summary**

# IV Summary

- A novel efficient search strategy that dramatically accelerates feature based registration.
  - speedup (~1000-fold) allows to carry out an exhaustive search for correspondences, in contrast with truncated local searches.
- A novel algorithm for robust estimation of an alignment transformation.
- Results are shown of TEM images of neural ultrastructure with increased accuracy and efficiency.
- Algorithm extensions and evaluation of randomized projection for dimensionality reduction.
  - Comparison of dimension reduction techniques, evaluation of dimensionality reduction that can be sustained while maintaining accuracy, an evaluation of the impact on distance distortion.

# References

- Achlioptas, D. (2003), “Database-friendly random projections: Johnson-Lindenstrauss with binary coins”, *J. of Computer and System Sciences* 66, 671–687
  - Andoni A. , Indyk, P. (2008), “Near-Optimal Hashing Algorithms for ANN in High Dimensions”, *Communications of the ACM*, vol. 51, no. 1, p. 117-122.
  - P.J. Besl and N.D. McKay. A method for registration of 3D shapes. *IEEE PAMI*, 14(2):239–256, 1992.
  - Brunelli R. and Poggio T. (1997) “Template Matching: Matched Spatial Filters and Beyond” ,*Pattern Recognition*, 30,5,751 - 768.
  - Dauguet, J., et al. (2007). “Alignment of Large Image Series using Cubic B-splines Tessellation: Application to Transmission EM Data.” *MICCAI 2007*.
  - Granger S., Pennec, X (2002) “Multi-scale EM-ICP, A Fast and Robust Approach for Surface Registration“. *ECCV (4)* 418-432
  - Horn, B. K. P., (1987) “Closed-form solution of absolute orientation using unit quaternions”, *Journal of the Optical Society of America Vol. 4*, 629-642.
  - Indyk, P. Motwani, R. (1998) “ANN: towards removing the curse of dimensionality”, 30th , *Annual ACM Sym. on Theory of Comp.*, Dallas, TX, ACM, NY, pp. 604–613.
  - Johnson, W.B. Lindenstrauss, J. (1984) “Extensions of Lipschitz mappings into a Hilbert space”, *Contemp Math*,26: 189–206.
  - P. Koshevoy, T. Tasdizen, R. Whitaker, B. Jones, and R. Marc, “Assembly of large three-dimensional volumes from serial section TEM,” *MICCAI*, 2006.
  - Ourselin, S. , et al. (2000) “Reconstructing a 3D structure from serial histological sections”, *Image and Vision Computing* 19 25–31
-

# References

- Blow, N (2007). “Following the wires.” Nature Methods 4 (11): 975-980.
- Denk, W., and H. Horstmann. (2004). “Serial block-face scanning electron microscopy to reconstruct three-dimensional tissue nanostructure.” PLoS Biol 2 (11):e329.
- Smith, S. J. (2007). “Circuit reconstruction tools today”. Curr Opin Neurobiol 17 (5):601-8.
- Courchesne E., et al. (2007) “Mapping Early Brain Development in Autism”, neuron.